

Evaluation of a resin-bonded graphite auxiliary electrode for sealed lead/acid batteries

Katsuhiko Takahashi

Matsushita Battery Industrial Co. Ltd., Technical Laboratory, Matsuhita-cho 1 Moriguchi, Osaka 570, Japan

Received 29 January 1996; revised 27 February 1996; accepted 8 March 1996

Abstract

A study is made of the hydrogen oxidation performance of partially-immersed resin-bonded graphite electrodes used as auxiliary electrodes for sealed lead/acid batteries. Cyclic voltammetry has been used to obtain certain information on the design of these strongly water-repellent auxiliary electrodes. Considering that, in an actual battery system, the auxiliary electrode is protected from oxygen evolution by a non-linear resistor, the potential is swept dynamically in a range from hydrogen potential to oxygen adsorption potential. The peak current value in each sweep cycle increases to a saturated value with cycling. This saturated value provides some information on the amount of catalyst, amount of resin, and other production conditions such as moulding pressure and sintering temperature. As a result of this investigation, important information is obtained for the design and improvement of auxiliary electrodes.

Keywords: Graphite; Electrodes; Lead/acid batteries; Hydrogen oxidation evolution

1. Introduction

Sealed lead/acid batteries using partially immersed auxiliary electrodes are well known [1–4]. Recent developments include the utilization of valve-regulated lead/acid battery technology to provide maintenance-free batteries. Auxiliary electrode systems are also convenient for application in anti-monny-type industrial lead/acid batteries.

Ruetschi and Ockerman [4] have reported a system where a catalytic auxiliary electrode is connected to the main electrode via a diode. Fukuda and Miura [5] used a special varistor in place of the diode as a non-linear resistor. This system was applied to large industrial lead/acid batteries in Japan, in 1967. Utilizing diodes or other non-linear resistors prevents gas from evolving at the auxiliary electrode and greatly increases the stability of the auxiliary electrode.

One further technology is vital for auxiliary electrodes, namely, the catalyst. Platinum is an excellent catalyst, but it is expensive. Reducing the required amount of platinum and extending the life of the auxiliary electrode are important themes in making the system a practical proposition.

In order to avoid the instability of carbon electrodes with platinum catalysts, new materials such as tungsten carbide have been investigated as platinum replacements [6]. Nevertheless, carbon is still a low-cost carrier and platinum is an excellent catalyst for electrochemical oxidation of hydrogen.

Thus, if an appropriate graphite and a resin with good water repellence can be found, resin-bonded electrodes can serve as excellent auxiliary electrodes.

In this study, amorphous graphite has been selected as a stable catalyst carrier, with fluororesin powder as a water-repellent binder. There are reports of auxiliary electrodes for sealed lead/acid batteries that utilize polytetrafluoroethylene (PTFE) in a resin-bonded electrode [1–4]. This combination is already popular in fuel cell technology. The structure of the resin-bonded electrode and the role of the resin in gas diffusion has been discussed in detail [7], but not specifically with respect to auxiliary electrodes.

The resin-bonded auxiliary electrodes are generally strongly water repellent and have a large electrical resistance. Furthermore, the auxiliary electrodes are used in sealed battery systems under partially-immersed conditions and the reaction site probably changes with time as the battery is used. This situation makes it difficult to produce auxiliary electrodes that have consistent performance. Therefore, pre-discharging techniques are used frequently before commencing evaluation studies [4,6,7]. Such techniques have been tried in this work, but since a strongly water-repellent resin-bonded electrode has a relatively weak hydrogen oxidation performance during the early stages, there is a danger of damaging the electrode if a large current is used. It takes a long time to reach a stable stage and the actual time required

varies greatly from electrode to electrode. Considering these points, cyclic voltammetry was applied to the fresh samples that were not subjected to any pretreatment.

Since an auxiliary electrode electrode is protected by a non-linear resistor, the potential was scanned in a hydrogen gas flow from higher than the hydrogen potential to slightly lower than the potential at which oxygen evolves.

In a practical system, the auxiliary electrode is exposed to a mixture of hydrogen and oxygen. Because of the corrosion of the positive electrode grid, the gas composition in the cell always tends towards a surplus of hydrogen [6]. Thus, the electrochemical oxidation of hydrogen is also investigated.

2. Experimental

The resin-bonded electrodes were prepared as follows. First, since an auxiliary electrode must be able to withstand the heat generated by the chemical catalyst reaction that occurs in the mixture of hydrogen and oxygen gases, graphites with good thermal stability were selected as catalyst carriers. Amorphous graphite was the best choice as it is easy to mould. The graphite powder was washed in a 6 N HCl solution, then rinsed in water and dried. Next, the dried cake was

crushed into a powder that could pass through a 100 mesh sieve.

The graphite was catalyzed by the formaline reduction method. First, the graphite was mixed with a chloroplatinic acid solution to form a slurry. Next, the slurry was dried and the resulting cake was reduced for 30 min at 50 °C in a mixture of 40% KOH and formaline. After adding the catalyst, the graphite was washed, crushed and powdered so that it could pass through a 100 mesh sieve.

N-10X (manufactured by Daikin) was selected on the water-repellent binder because it has an appropriate level of water-repellence and is easy to a mould. N-10X is a powdered copolymer of PTFE and polyhexafluoropropylene (PHFP). The binder contributed between 15 and 25 wt.% of the total weight of the moulding. The resin and the graphite powder carrying the catalyst were mixed as dry powders. Acetylene black or other powdered materials were added at this stage, if required.

13.2 g of the mixed powder was moulded by a programmed force of between 125 and 170 kg cm⁻², using a stainless-steel mould with hole of approximate dimensions 50 mm × 60 mm. The resulting cake was heat-treated in a flow of nitrogen to sinter the resin. The sintering temperature was set in the range 200 to 360 °C, i.e. lower than the melting point of the

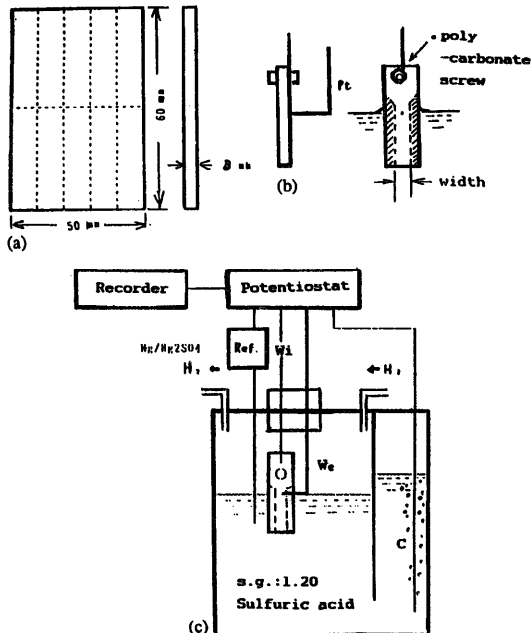


Fig. 1. (a) Moulded plate, (b) test electrode, and (c) test cell.

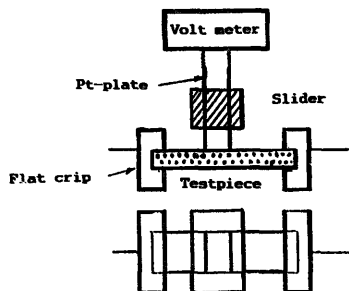


Fig. 2. Method for measuring the electric resistance.

resin (380 °C). The resulting sintered plate was approximately 3 mm thick. Test pieces were then cut to the desired shapes, as shown in Fig. 1(a).

In order to examine electrochemical performance when partially immersed, 10 mm × 30 mm test pieces were prepared. A small hole was made near the top of the test piece to accommodate the current lead. This was a platinum wire that was secured by a polycarbonate screw, and shown in Fig. 1(b). To measure the working potential, a platinum needle probe was inserted close to the meniscus. If it was necessary to reduce the size of the sample close to the meniscus, the test piece was cut along the dotted lines shown in Fig. 1(b).

Cyclic voltammetry was used as the main evaluation method. The test cell is shown in Fig. 1(c). Hydrogen gas

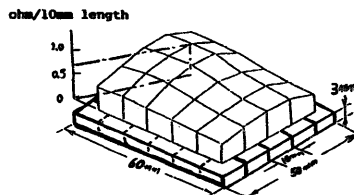


Fig. 3. An example of electric resistance distribution. Sample consisting of graphite, 1 wt.% acetylene black, 5 wt.% Pt, and 15 wt.% resin; moulding pressure: 141 kg/cm²; sintering temperature: 300 °C, and thickness: 3 mm.

was passed through the gas space in the cell. In order to prevent the meniscus position from being disturbed by hydrogen gas evolving from the counter electrode, the latter was located outside the main compartment of the cell. A potentiostat (HA-305, by Hokuto Denko) was used to determine electrode performance.

When a sealed battery is actually operating, the auxiliary electrode is exposed to a wide range of potential in a mixture of hydrogen and oxygen gases. A non-linear resistor, such as a diode, can protect the auxiliary electrode from oxygen evolution. Accordingly, the operating range of potential was set from 0 to 1.70 V with respect to the hydrogen potential, which corresponds to -0.65 to 1.03 V against a Hg/Hg₂SO₄ reference electrode. Various potential scan rates were tried, the most efficient was 30 s/V.

In order to discover the level of electric resistance that would influence the electrode performance, the sintered

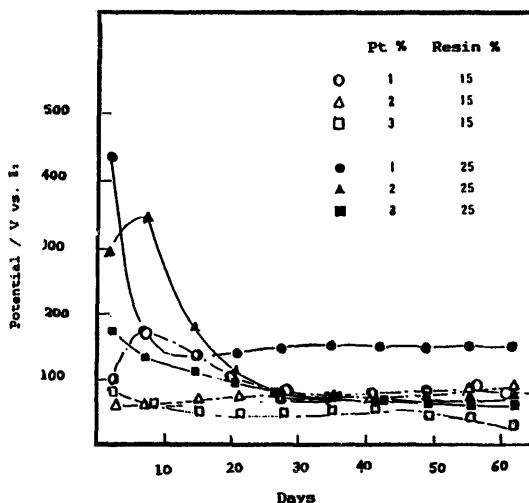


Fig. 4. Transition of hydrogen oxidation potential during pre-discharge operation. Samples: resin-bonded graphite with platinum moulding pressure: 141 kg/cm²; sintering temperature: 300 °C; width: 10 mm; thickness: 3 mm; electrolyte: H₂SO₄ (1.20 sp. gr.), and current: 50 mA.

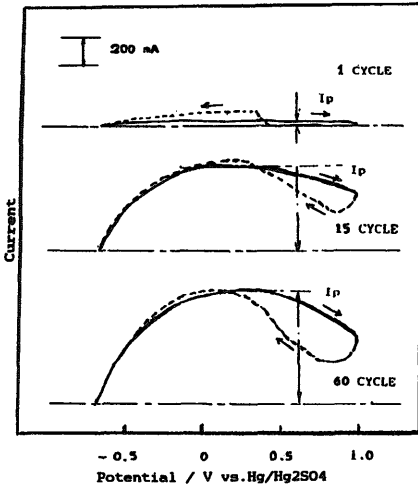


Fig. 5. Current-potential curve for different cycles. 3 wt.% Pt, 20 wt.% resin; moulding pressure: 141 kg/cm²; sintering temperature: 300 °C; width: 6 mm; thickness: 3 mm; sweep rate 30 s/V; sweep range: -0.67 to 1.03 V vs. Hg/Hg₂SO₄.

plate's electrical resistance and its distribution were measured in the same direction as the flow of current. The sintered plate was cut into 10 mm × 60 mm test pieces. The normal four-point instrument for measuring resistance could not be used

because the probes penetrated into the soft surface of the plate. Therefore, a special tool (Fig. 2) was custom-made to take the measurements.

3. Results and discussion

3.1. Electrical resistance and its distribution

An example of the distribution of electrical resistance in the resin-bonded electrode plate is shown in Fig. 3. The sample included 5 wt.% platinum, 25 wt.% resin and 1 wt.% acetylene black. The value on the vertical axis of each square position in the figure shows the resistance value measured every 10 mm along the length of a 3 mm thick, 50 mm wide testpiece. The maximum value was 0.65 Ω and the minimum value was 0.38 Ω. A similar sample without acetylene black gave a maximum value some 15% higher and with a distribution profile that was very similar to the sample shown. It is considered that these distribution profiles result not from the inherent properties of the materials themselves but from filler irregularities and flaws in the mould.

Resin-bonded substances generally display high resistance. If there is a long distance from the current connector to the meniscus region, the current-potential curve shifts to the higher potential side [4]. Consequently, the level can be estimated from these resistance values. This means that positioning the potential measurement probe close to the meniscus is an effective way of avoiding the influence of the measurement on the electrochemical performance. These electric resistances together with the non-linear resistor's

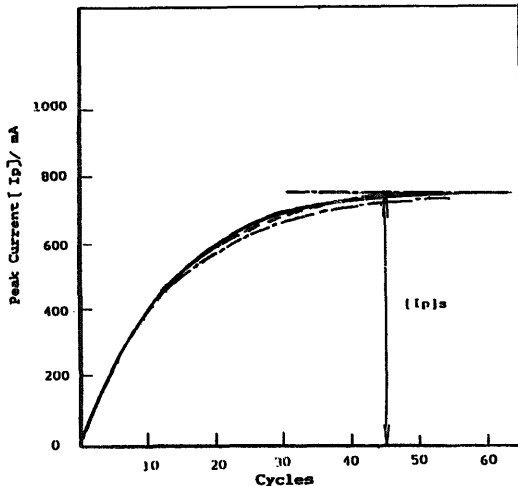


Fig. 6. Transition of peak current (I_p). The three samples were cut out from the plate used to provide data in Fig. 5.

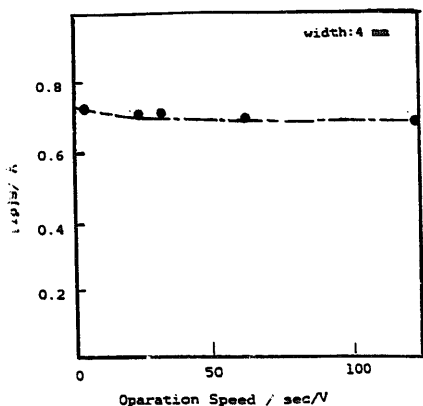


Fig. 7. Relation between potential operation speed and (I_p) . 3 wt.% Pt 25 wt.% resin; pressure: 141 kg/cm²; sintering temperature: 360 °C.

resistance can be used to determine the potential close to the meniscus. Thus, the resistance value is a useful reference when designing the width of electrode to give an appropriate potential close to the meniscus.

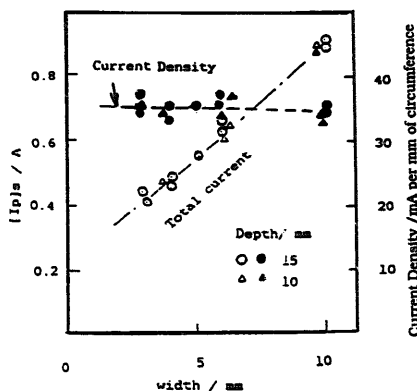


Fig. 8. Relation between sample width at meniscus position and (I_p) , at different immersed depths; operation speed: 30 s/V.

3.2. Problems with small current pre-operation

Before commencing the main evaluation test of a gas-diffusion electrode, pre-operation with small currents was attempted for electrodes with different fluoro-resin and plat-

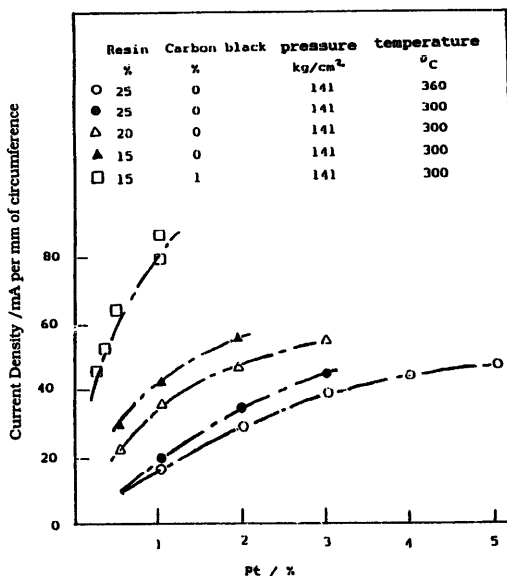


Fig. 9. (I_p) , for electrodes with different contents of Pt and resin. (I_p) is shown as current density per unit circumference length. Range: -0.67 to 1.03 V vs. Hg/Hg₂SO₄; sweep rate: 30 s/V.

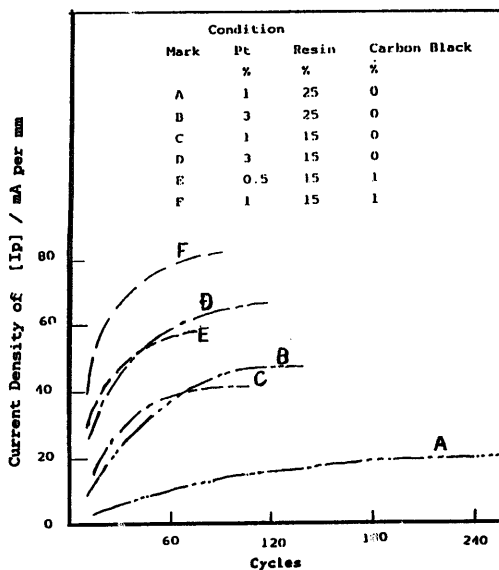


Fig. 10. Transfer of (I_p) on the electrodes with different Pt and resin contents; operating condition as shown in Fig. 9.

inum contents. The transition in potential during the test using small current is shown in Fig. 4. The oxidation current was set at 50 mA per 10 mm width at the meniscus. The results showed that, for samples with a strong resin bonding, a long period (approximately 1 month) was required for the potential to stabilize, and that there were large variations between individual samples. Such behaviour makes it difficult to decide what should be compared and at which point. A more rapid and more reproducible method of evaluating auxiliary electrode performance is required.

3.3. Cyclic voltammetric tests

Cyclic voltammetry was used to evaluate the resin-bonded graphite test piece. Preliminary experiments showed that there was a risk that the oxidation current would exceed the operating range of the apparatus. Therefore, the width of the test piece close to the meniscus was reduced to 4 mm, as shown in Fig. 1. The electrolyte was dilute sulfuric acid (1.20 sp. gr.), as generally used in large industrial batteries.

The initial sample was manufactured with the following conditions: 3 wt.% platinum, 20 wt.% resin, moulding pressure 141 kg/cm², and sintering temperature 300 °C. The typical current–potential relationship at several points during cycling is presented in Fig. 5. In the early stage of the work, it was difficult to determine the performance.

After several cycles, however, a current–potential curve that peaked between 0 and 0.3 V higher than the reference electrode clearly emerged. The peak current in each cycle was designated (I_p), and the relationship between (I_p) and the number of cycles was expressed as shown in Fig. 6. It can be seen that (I_p) increases with the number of cycles and, after several tens of cycles, tends to approach a constant saturation value (I_p)_s. Similar results were obtained from two or three different samples taken from the same sintered plate. This confirms good reproducibility for the rate of increase in both (I_p) and (I_p)_s.

3.4. Effect of experimental conditions

The depth of test piece immersion, the shape of the test piece close to the meniscus, and the potential driving speed were investigated to discover their effect on (I_p)_s.

As first, the depth of immersion was fixed at 15 mm, and the width of the test piece at the meniscus was fixed at 6 mm.

After (I_p) reached saturation with a driving speed of 30 s/V, the speed was varied to obtain its relationship with (I_p)_s. The results are shown in Fig. 7. (I_p)_s is only slightly influenced by the driving speed. The rate of increase in (I_p) corresponds to the total test time rather than to the number of cycles. Of the various speeds investigated, 30 s/V gave very good reproducibility and a rapid result. In fact, it was so rapid

that a test of 100 cycles could be completed in only 170 min. This was sufficient to complete a test of one sample.

The relationship between $(I_p)_s$ and test piece width is given in Fig. 8. The results obtained by alternating the depth of partial immersion of the test piece between 10 and 15 mm are also shown. Within this range, $(I_p)_s$ is basically unaffected by depth, but varies in direct proportion to the test piece width. The auxiliary electrodes use large amounts of strongly-bonding resin, so this result is thought to be due to the fact that the location of the main reaction site is close to the meniscus near the electrode surface, rather than in gas channels within the electrode. The values for $(I_p)_s$ obtained in these experiments are also expressed in terms of current density per unit length of electrode perimeter at the meniscus. These data are also plotted in Fig. 8. It is seen that such current density is virtually constant, and confirms that the results are affected by the length of the perimeter at the meniscus rather than by the width of the test piece. Thus, $(I_p)_s$ values for test pieces of different widths can be compared by converting to current density per unit meniscus length.

3.5. Evaluation of production conditions

Production conditions such as the amount of catalyst and resin, the moulding pressure and the sintering temperature were investigated by evaluating test pieces manufactured under different conditions.

The relationship between the amount of platinum and $(I_p)_s$ is given in Fig. 9. $(I_p)_s$ is expressed in terms of current density/unit meniscus length. The results show that although $(I_p)_s$ is influenced by the amount of platinum, it depends to a far greater extent on the amount of resin and on the addition of acetylene black. Acetylene black is mixed with the catalyst-carrying graphite in the form of a powder, so it is unlikely that a chemical change occurs during catalysis.

The changes in (I_p) up to the saturation point, $(I_p)_s$, are shown in Fig. 10. The behaviour of test pieces with added acetylene black resembles that of test pieces with reduced amounts of resin. Similarly, Fig. 11 shows transitions in (I_p) for variations in: (i) moulding pressure, and (ii) sintering temperature. The optimum values appear to be 125 kg/cm² for moulding pressure and 300 °C for sintering temperature.

The above results show that the rate of increase tends to accelerate when conditions are changed so as to reduce the bonding strength of the resin or to lower the water-repellence. The means that structural factors such collapse of the bonding structure and changes in water repellence may have an influence on (I_p) . Above a certain level of structural change, effects due to the catalyst itself become indistinguishable.

Test pieces moulded with a high pressure of 170 kg/m² are physically strong. (I_p) measurements for such test pieces increase rapidly but stabilized at a low saturation point. If sintering is performed at 200°C, the plate is softer and the binding forces are weaker. Rise time is fast but (I_p) starts to drop soon after the saturation point is reached. There is a

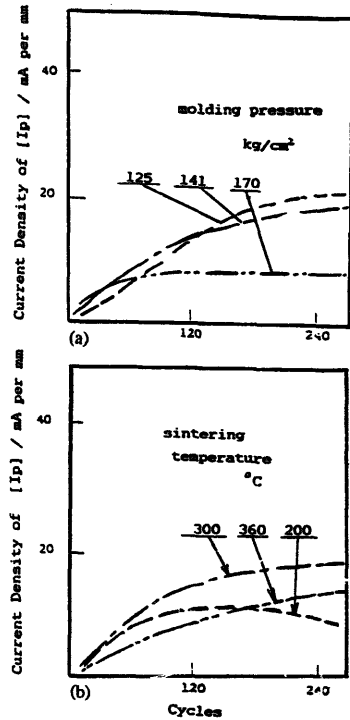


Fig. 11. Effect of different process conditions on (I_p) ; operating conditions as shown in Fig. 9. (a) Effect of moulding pressure: 1 wt.% Pt; 25wt.% resin; sintering temperature: 300 °C. (b) Effect of sintering temperature: 1 wt.% Pt; 25 wt.% resin; moulding pressure: 141 kg/cm²

possibility that the drop in (I_p) after saturation may provide some information on the physical degradation and life.

4. Conclusions

By applying cyclic voltammetry to evaluate resin-bonded auxiliary electrodes the following four conclusions have been reached:

- (i) (I_p) and its saturated value $(I_p)_s$ provide information on the hydrogen oxidation performance of an auxiliary electrode;
- (ii) $(I_p)_s$ corresponds to the added platinum content;
- (iii) $(I_p)_s$ is influenced greatly by structural factors such as the amount of resin, the addition of acetylene black, the moulding pressure, and the sintering temperature, and
- (iv) transitions in (I_p) may provide information on physical changes such as water repellence and bonding strength.

It was also concluded that the cyclic voltammetric technique provides a rapid method of evaluating relative characteristics of resin-bonded auxiliary electrode and a good deal of useful information on auxiliary electrode design and manufacture.

Acknowledgements

The author wishes to thank Professor Dr H. Iwahara of the Centre for Integrated Research in Science and Engineering, Nagoya University for his useful advice and comments.

References

- [1] R.F. Nelson, *J. Power Sources*, 31 (1990) 3.
- [2] R. Ruetschi, *J. Power Sources*, 2 (1977/78) 3.
- [3] P. Ruetschi and B.D. Cahan, *US Patent No. 308 0440* (1963).
- [4] P. Ruetschi and J.B. Ockerman, *Electrochem. Technol.*, 14 (1966) 7–8.
- [5] M. Fukuda and T. Miura, *US Patent No. 3 658 591* (1972).
- [6] G. Papazov, L. Nikolov, D. Pavlov, P. Andreev and M. Bojinov, *J. Power Sources*, 31 (1990) 79.
- [7] M. Watanabe, M. Makita, H. Usamiand and S. Motoo, *J. Electroanal. Chem.*, 197 (1986) 195.